

1 Carbon flux and forest dynamics: increased deadwood
2 decomposition in tropical rainforest tree-fall gaps
3

4 **Running title:** Faster deadwood decay in canopy gaps
5

6 **Authors:** H. M. Griffiths¹, P. Eggleton², N. Hemming-Schroeder³, T. Swinfield^{4,5}, J. S.
7 Woon^{1, 2}, S. D. Allison^{3,6}, D.A. Coomes⁴, L. A. Ashton⁷ & C. L. Parr^{1,8,9}
8

9 **Affiliations**

10 ¹ School of Environmental Sciences, University of Liverpool, Liverpool, L69 3GP, UK

11 ² Department of Life Sciences, Natural History Museum, London, UK

12 ³ Department of Earth System Science, University of California, Irvine, CA 92697, USA

13 ⁴ Department of Plant Sciences, University of Cambridge Conservation Research Institute, Pembroke
14 Street, Cambridge, CB2 3QZ, UK

15 ⁵ Centre for Conservation Science, Royal Society for the Protection of Birds, David Attenborough
16 Building, Pembroke Street, Cambridge, CB2, 3QZ, UK

17 ⁶ Department of Ecology and Evolutionary Biology, University of California, Irvine, CA 92697, USA

18 ⁷ School of Biological Sciences, The University of Hong Kong, Hong Kong SAR, China

19 ⁸ Department of Zoology & Entomology, University of Pretoria, Pretoria, South Africa

20 ⁹ School of Animal, Plant and Environmental Sciences, University of the Witwatersrand, Wits, South
21 Africa

22

23 Hannah Griffiths ORCID: 0000-0002-4800-8031

24 **Contact information**

25 Email: Hannah.griffiths@liverpool.ac.uk; Tel: +44 151 794 2000

26 **Abstract**

27 Tree mortality rates are increasing within tropical rainforests as a result of global
28 environmental change. When trees die, gaps are created in forest canopies and
29 carbon is transferred from the living to deadwood pools. However, little is known about
30 the effect of tree-fall canopy gaps on the activity of decomposer communities and the
31 rate of deadwood decay in forests. This means that the accuracy of regional and global
32 carbon budgets is uncertain, especially given ongoing changes to the structure of
33 rainforest ecosystems. Therefore, to determine the effect of canopy openings on wood
34 decay rates and regional carbon flux, we carried out the first assessment of deadwood
35 mass loss within canopy gaps in old-growth rainforest. We used replicated canopy
36 gaps paired with closed canopy sites in combination with macroinvertebrate
37 accessible and inaccessible woodblocks to experimentally partition the relative
38 contribution of microbes versus termites to decomposition within contrasting
39 understory conditions. We show that over a 12-month period, wood mass loss
40 increased by 63% in canopy gaps compared with closed canopy sites and that this
41 increase was driven by termites. Using LiDAR data to quantify the proportion of canopy
42 openings in the study region, we modelled the effect of observed changes in
43 decomposition within gaps on regional carbon flux. Overall, we estimate that this
44 accelerated decomposition increases regional wood decay rate by up to 18.2%,
45 corresponding to a flux increase of $0.27 \text{ Mg C ha}^{-1} \text{ yr}^{-1}$ that is not currently accounted
46 for in regional carbon budgets. These results provide the first insights into how small-
47 scale disturbances in rainforests can generate hotspots for decomposer activity and
48 carbon fluxes. In doing so, we show that including canopy gap dynamics and their

49 impacts on wood decomposition in forest ecosystems could help improve the
50 predictive accuracy of the carbon cycle in land surface models.

51

52 **Key words**

53 Termites; Invertebrates; Carbon cycling; Carbon modelling; Canopy gap; Tree
54 mortality; Disturbance; Global change

55

56 **Introduction**

57

58 Uncertainty in the behaviour of the carbon cycle is one of the biggest limiting factors
59 in accurately predicting Earth's temperature into the 21st century (Bodman, Rayner, &
60 Karoly, 2013). Tropical forests hold over half of global forest carbon stocks (471 ± 93
61 PgC), 56% of which is stored in biomass, and sequester 1.2 ± 0.4 PgC annually (Pan
62 et al., 2011). Recent work has highlighted how human pressures affect rainforest
63 carbon stocks in living and dead biomass, showing that selective logging and
64 degradation increase the proportion of deadwood stocks relative to living biomass in
65 African and Asian rainforests (Carlson, Koerner, Medjibe, White, & Poulsen, 2017;
66 Pfeifer et al., 2015).

67

68 Decomposition is the process by which the carbon in dead plant material is assimilated
69 into soil carbon stores, lost through leaching or released as CO₂ into the atmosphere
70 through respiration (Cornwell et al., 2009; Swift, 1977). Yet, despite the fact that
71 decomposition has far reaching implications for global carbon budgets (Hubau et al.,
72 2020), it remains poorly understood compared with other key ecosystem processes
73 such as primary production (Harmon, Bond-Lamberty, Tang, & Vargas, 2011).
74 Furthermore, what is known about the factors controlling deadwood decay is
75 geographically biased towards temperate regions, with tropical forest decomposition
76 studies representing just 14% of the published literature (Harmon et al., 2020). This
77 bias means we lack a basic understanding of the factors that mediate the rate and fate
78 of carbon turnover through globally important deadwood stocks in tropical rainforests.

79

80 The effect of canopy openness represents an important source of uncertainty in our
81 understanding of the factors that affect the decomposition of deadwood in forests
82 (Harmon *et al.*, 2020). This is a major gap in understanding given that tree mortality
83 rates are rising in humid tropical forests (McDowell *et al.*, 2018) as a result of increases
84 in the frequency and severity of hurricanes and drought (Cai *et al.*, 2014); continued
85 selective logging and degradation (Baccini *et al.*, 2017); and increases in biotic agents
86 of tree death (liana load, insect outbreaks and disease; Allen, Breshears & McDowell
87 2015). Consequently, it is likely that the size and frequency of rainforest canopy gaps
88 are increasing, along with concurrent changes in the volume and spatial distribution of
89 deadwood stocks (Carlson *et al.*, 2017; Pfeifer *et al.*, 2015). However, because our
90 knowledge of the effect of canopy gaps on deadwood decay rates is currently limited
91 to just two studies in temperate and boreal forests (Janisch, Harmon, Chen, Fasth, &
92 Sexton, 2005; Shorohova & Kapitsa, 2014), we lack an empirical evidence base from
93 which to predict the consequences of ongoing changes to the structure of tropical
94 rainforests for decomposition and carbon flux. Data shortages such as these limit the
95 capacity to resolve carbon budget imbalances because information on how land-
96 surface heterogeneity can affect carbon-cycling and land-atmosphere interactions is
97 a key area of uncertainty in Earth system models (Lawrence *et al.* 2019). Therefore,
98 there is a clear need to improve our mechanistic understanding of the drivers of
99 change in rainforest carbon budgets and thus increase the accuracy and predictive
100 power of the land surface models included in Earth system models.

101
102 There is mounting evidence that termites along with microbes are the major agents of
103 deadwood decomposition in rainforest ecosystems (da Costa, Hu, Li, & Poulsen, 2019;

104 Griffiths, Ashton, Evans, Parr, & Eggleton, 2019; Liu et al., 2015). It is possible that
105 treefall canopy gaps could negatively or positively affect the activity of both groups.
106 Habitat disturbance and degradation reduces termite abundance and diversity (Dibog,
107 Eggleton, Norgrove, Bignell, & Hauser, 1999; Eggleton et al., 1995; Ewers et al., 2015;
108 Luke, Fayle, Eggleton, Turner, & Davies, 2014; Tuma et al., 2019) while microbial-
109 mediated nutrient mineralisation rates decline in response to drought (Yavitt, Wright,
110 & Wieder, 2004). Changes to the structure of forests caused by removal of trees during
111 selective logging has been reported to increase microclimate heterogeneity and create
112 hotter and drier conditions in the forest understory (Blonder et al., 2018; Hardwick et
113 al., 2015). Therefore, the changes in understory conditions caused by openings in the
114 canopy when a tree dies could have major negative effects on both termite and
115 microbial mediated decomposition. If this is the case, we expect decay rates to slow
116 in canopy gaps as result of disturbance and unfavourable microclimatic conditions for
117 the decomposer community. However, an alternative possibility is that the high
118 concentration of foraging resource (i.e. dead plant matter) in canopy gaps, that result
119 from tree death, may positively affect decomposition processes by attracting termites
120 and/or stimulating a positive priming effect within the microbial community (e.g. Lyu et
121 al., 2018). Under this scenario, we expect to see an increase in decay rates in canopy
122 gaps in response to elevated resource availability where a tree has fallen.

123

124 The overarching aim of this investigation was to determine if deadwood decay rates
125 differ in canopy gaps compared with closed canopy sites in tropical rainforest.
126 Additionally, we partitioned the relative contribution of microbes and termites in driving
127 deadwood mass loss in canopy openings and estimated the effect of any changes in

128 decomposition rates within canopy gaps on regional carbon flux. To achieve this aim,
129 we used macroinvertebrate-accessible and inaccessible woodblocks placed within
130 tree fall canopy gaps and closed canopy sites in an old growth rainforest in Malaysian
131 Borneo. Furthermore, we assessed the termite community composition and soil
132 microclimatic conditions within experimental sites and estimated the volume of
133 deadwood associated with canopy gaps compared with closed canopy sites. This
134 unique experimental design allowed us to the test alternative hypotheses that
135 deadwood decomposition in canopy gaps could either: 1) decelerate due to a negative
136 effect of disturbance and a hotter, drier microclimate (e.g. Blonder *et al.* 2018) leading
137 to a reduction in the activity of the decomposer community, or 2) accelerate in
138 response to an influx of dead plant material attracting termite foraging activity and/or
139 stimulating a microbial priming effect (e.g. Lyu *et al.* 2018). To scale up our results and
140 place them in a regional context, we used remote sensing (LiDAR) data to quantify the
141 proportion of canopy openings in the study region and modelled the effect of observed
142 changes in decomposition within gaps on regional carbon flux.

143

144 **Materials and methods**

145 *Study site and gap selection*

146 This study was carried out within an area of lowland, old growth dipterocarp rainforest
147 in the Maliau Basin Conservation Area, Sabah, Malaysia ($4^{\circ} 44' 35''$ to $55''$ N and 116°
148 $58' 10''$ to $30''$ E; mean annual rainfall $2838 \text{ mm} \pm 93 \text{ mm}$). On the 20th of July 2017,
149 there was a storm at the study site, which generated winds speeds of 8.4 m/s (Fig.
150 S1). These were among the strongest winds normally experienced in inland forests of
151 the region, which placed extreme sheer stress on trees (Jackson *et al.*, 2020).

152 Consequently, a large number of trees fell within the same 24-hour period in the study
153 location. Ten tree-fall gaps (mean length: $32\text{ m} \pm 2.8$, mean width: $24.5\text{ m} \pm 3$; see
154 table S1 for gap characteristics) created during this event were selected for use in this
155 investigation, along with ten adjacent closed canopy sites, located 20 m from the edge
156 of each gap. We took 10 hemispherical photos in each gap and closed canopy sites
157 to quantify canopy openness at each location (see below).

158

159 *Decomposition assay*

160 In October 2017, we established a wood decomposition assay. Using a termite
161 suppression experiment combined with macroinvertebrate accessible and
162 inaccessible mesh bags, Griffiths *et al.* (2019) demonstrated that non-termite
163 macroinvertebrates did not contribute significantly to the decomposition of a
164 standardised wood substrate, *Pinus radiata* blocks, at this site. Therefore, to assess
165 the rate of decomposition within these paired gap and closed canopy sites and
166 determine the relative contributions of termites versus microbes to the process, we
167 used the same assay of mass loss from untreated *P. radiata* wood within
168 macroinvertebrate accessible and inaccessible bags. Wood blocks ($9 \times 9 \times 5\text{ cm}$, 161.2
169 $\pm 1.3\text{ g}$; wood density of 0.40 g cm^{-3} [Zanne *et al.*, 2009]; wood C:N ratio of 462 ± 48
170 [Ganjegunte, Condron, Clinton, Davis, & Mahieu, 2004]) were dried at $60\text{ }^{\circ}\text{C}$ until they
171 reached a constant weight and placed inside “open” (accessible to
172 macroinvertebrates, principally termites, and microbes), or “closed” (accessible to
173 microbes only) bags, which were all made with 300 micron nylon mesh (Plastok™,
174 Merseyside, UK). The open woodblocks had ten 1 cm holes cut into the top and bottom
175 of the bags to avoid confounding effects of using mesh of different sizes in

176 decomposition assays (Stoklosa et al., 2016). The edges of the closed bags were
177 folded several times and sealed with staples to prevent access by invertebrates. In
178 each gap and closed canopy site, we ran a 50-m transect and randomly placed 5 open
179 and 5 closed wood blocks 5 m apart along the transect ($n = 10$ per site; $n = 200$
180 woodblocks in total: $10 \times$ forest sites \times 2 canopy treatments [closed canopy or gap] \times
181 2 mesh treatments [open or closed] \times 5 replicates). Because the gaps were irregular
182 in shape (Appendix table S1), we placed the transects along the longest axis of each
183 gap. In all but one of the gap sites, we were unable to establish a 50 m transect,
184 therefore, we placed an additional line perpendicular to the first, ensuring that each
185 block was always at least 5 m apart from its nearest neighbouring block (Fig. 1).

186

187 A hemispherical photograph was taken by placing an iPhone 6 with a fisheye lens
188 attachment directly on top of each wood block. Photographs were analysed using the
189 function *Hemiplot* in R to calculate canopy openness, which was twice as high within
190 the gaps compared with closed canopy sites ($t = 9.67$, $P < 0.001$, mean openness in
191 gap sites = 0.24 ± 0.03 ; mean openness in closed canopy sites = 0.12 ± 0.02 ; Fig.
192 S2). When placing the woodblocks, the top layer of leaf litter was removed, and the
193 blocks were put directly on the humus layer. Wood blocks were left on the forest floor
194 for 12 months (October 2017 to October 2018), after which they were collected and
195 dried at 60 °C until they reached a constant weight. Once dried, wood material was
196 separated from termite soil. The remaining deadwood and termite material (carton and
197 soil) was then re-weighed separately to calculate the proportion of mass loss from
198 each block and the mass of soil brought into the mesh bags by termites. Given that
199 termites are the only invertebrates known to translocate soil into deadwood (Oberst,

200 Lai, & Evans, 2016), the mass of soil moved into the experimental woodblocks
201 provides additional information on the termite activity compared with non-termite
202 wood-feeding invertebrates.

203

204 *Soil conditions and termite communities*

205 Every month for the 12-month duration of the study, soil moisture percentage and soil
206 temperature were measured within 5 cm of each wood block using a Delta-T Devices
207 HH2 moisture metre (precise to 0.01 %) and a digital soil thermometer. Measurements
208 were taken in dry conditions, between 8 AM and 10 AM. To assess termite
209 communities located within the gap and closed canopy sites, we carried out termite
210 transects in September 2018 using the Jones and Eggleton transect method (Jones &
211 Eggleton, 2000). This method uses a 100 m x 2 m belt transect which is divided into
212 twenty 5 m x 1 m sections. Each section is sampled for 30 minutes by two trained
213 collectors searching for termites in twelve 12 cm x 12 cm x 10 cm soil pits and
214 examining all dead wood, leaf litter and trees for the presence of termites. When
215 encountered, termite specimens were collected in 70% ethanol and taken to the
216 laboratory for identification. Because our gap sites were not big enough to place a 100
217 m transect, we carried out the same method but two using smaller transects to equal
218 a 50 m transect combined. Therefore the sampling effort was half that of the Jones &
219 Eggleton (2000) method.

220

221 *Quantifying regional gap area*

222 To assess the size and frequency of gaps within Maliau Basin Conservation Area, we
223 used LiDAR data collected from an airborne survey, which was carried out by the

224 Natural Environment Research Council (NERC) Airborne Research Facility (ARF). In
225 November 2014, a Dornier 228-201 was flown at 1,400-2,400 m a.s.l. with a ground-
226 based Leica base station running simultaneously to allow sub-meter accuracy and
227 georeferencing of the data. Light detection and ranging data were collected using a
228 Leica ALS50-II LiDAR sensor, which emits 120 kHz frequency pulses, has a 12° field
229 of view and a footprint of approximately 40 cm. See Swinfield et al. (2019) for details
230 of LiDAR data processing to generate canopy height and digital terrain models at a
231 0.5 m resolution. Using these data, we analysed canopy height models to identify
232 gaps, defined as areas with a canopy height of less than 5 m. Gaps larger than 1 ha
233 were filtered out to remove LiDAR artefacts, manmade clearances and the river
234 running through Maliau Basin. We used the package *landscapemetrics* in R and the
235 thresholds described above to detect gaps and to calculate the area of each. We then
236 filtered these results to select only gaps that were between 0.025 and 0.16 ha, which
237 is the area range of the gaps forming the basis of this investigation. This allowed us to
238 assess the total area and percentage of the landscape likely to be subject to similar
239 microclimatic conditions to our gap sites at the time of the airborne survey and to
240 quantify the percentage of gaps that are similar in size to those in this study.

241

242 *Dead wood surveys*

243 To estimate the volume of deadwood found on the forest floor in areas affected by
244 tree-fall, compared with undisturbed areas, we carried out deadwood surveys in
245 December 2017. To avoid disturbing our decomposition assays, these surveys were
246 carried out in areas within the forest surrounding experimental plots. We established
247 eight 50 m transects, four of which were within 5 m of a tree that had fallen during the

248 storm in July 2017 and four that were in areas of forest at least 20 m from the nearest
249 tree fall. Along each transect, we recorded the diameter of each piece of deadwood
250 that intersected with the line, and these values were used to calculate the volume of
251 dead wood using the following equation (Van Wagner 1968):

252

253

$$V = \frac{\pi^2}{8L} \sum d^2$$

254

255 Where V is the volume of deadwood (cm³/50 m), d is the diameter of the deadwood
256 item at the intersection and L is the length of the sample line.

257

258 **Carbon Modelling**

259 A bootstrapping scheme with a million simulations was implemented to estimate the
260 carbon flux from dead wood and its uncertainty in Maliau Basin. We estimated carbon
261 fluxes for a completely closed canopy scenario versus scenarios with observed
262 changes in decay rate and deadwood volume in canopy openings as well as canopy
263 gap percentages derived from the remote sensing analysis.

264

265 *Wood density*

266 One species, *Pinus radiata*, was used for estimating wood mass loss in our
267 experiment. Therefore, to account for diversity in wood traits of other species likely to
268 occur at the study site, we used tree survey data from Newbery and Lingenfelder
269 (2004) (collected from a lowland dipterocarp forest site within 100 km of our study site).
270 Our bootstrap analysis used the tree species frequencies from Newbery and
271 Lingenfelder (2004) and selected a wood density for each species from the Global

272 wood density database (Zanne et al., 2009). Where wood density for a species was
273 not available, we randomly selected a wood density value from members of the same
274 genus within the same region category (South-East Asia (tropical)). A histogram of the
275 wood density distribution for this study is shown in Fig. S3. Given that termite and
276 microbial decay rate is negatively associated with wood density in tropical systems
277 (Liu et al., 2015; Mori et al., 2014), this approach reduces the possibility that our model
278 overestimates overall decay rate as a result of the disparity between the density of our
279 decomposition substrate (*P. radiata*: wood density of 0.40 g cm⁻³) and the estimated
280 median density of wood from trees in the study region (0.54 g cm⁻³). We note that the
281 relationship between wood density and decay rate is less clear in temperate forests
282 (Hu et al., 2018; Kahl et al., 2017). In addition to wood density, other traits, such as
283 wood stoichiometry and size of woody substrate (Hu et al., 2018; Kahl et al., 2017;
284 Oberle et al., 2020), are likely to influence decay rates. However, information is lacking
285 on how these other traits affect termite-mediated decay, or wood decomposition more
286 generally in tropical systems. Therefore, we did not incorporate these factors into our
287 models of regional carbon fluxes.

288

289 *Scaling decay rates*

290 Liu et al. (2015) is the only study we know of that quantifies how termite-mediated
291 decay rates depend on wood density. Therefore, we first built a model to represent
292 wood decay rates under termite attack based on Liu et al. (2015). We scaled this model
293 to represent wood decay in gaps using the *P. radiata* wood density and associated
294 decay rate from our study. Then, we scaled the model again to represent these rates
295 under the closed canopy. Wood decay rates in forest gaps were based on Liu et al.

296 (2015) who measured wood traits and decay rates driven by microbes and termites
297 for 66 species. We fitted an exponential model to decay rates as a function of wood
298 density using an L1 scheme that minimizes the sum of the absolute value of the
299 residuals (R package: *L1pack*) (Fig. S4). We used this scheme, rather than a least-
300 squares approach, to avoid over-weighting outliers with high decay rates. To obtain a
301 decay rate for each wood density value, we sampled from a normal distribution with
302 the decay rate model prediction as the mean and the 68%-confidence interval of the
303 model fit as the standard deviation (in log space). To avoid biologically unrealistic
304 decay rates, we truncated the model to the middle 96% of the modelled decay rate
305 estimates (Fig. S4). Because the model derived from Liu *et al.* (2015) predicted a much
306 higher mean decay rate for *P. radiata* than found in our study (1.3 year⁻¹ compared
307 with 0.49 year⁻¹), we scaled the model to reflect the *P. radiata* decay rates in the
308 canopy gaps open to termite activity that we measured in the field. To predict decay
309 rates under the closed canopy, we also scaled our gap model predictions to match the
310 decay rates of *P. radiata* open to termite decomposition under closed canopy in our
311 study. We accounted for random error in this scaling process by sampling our decay
312 rate dataset with $N(\mu=0.49, \sigma=0.05)$ for the forest gaps and $N(\mu=0.30, \sigma=0.04)$ for the
313 closed canopy to obtain a distribution of scaling factors. These normal distributions
314 were also truncated to the middle 96% quantile.

315

316 *Carbon fluxes*

317 To estimate the deadwood carbon pool at our study site, we used surveys from Pfeifer
318 *et al.* (2015) from nearby Old Growth plot (OG2) of the Stability of Altered Forest
319 Ecosystem (SAFE) project, located within Maliau Basin, <5 km kilometres from our

320 study sites. Pfeifer et al. (2015) estimated there to be 10.2 ± 3.5 Mg C per hectare
321 contained in deadwood at the OG2. For the bootstrapping scheme, we sampled 1×10^6
322 times from a normal distribution of wood pools with the corresponding mean and
323 standard deviation, truncated to the middle 96% quantile. We then estimated carbon
324 fluxes, F , for the closed canopy baseline scenario using the equation

325

326
$$F = k_{canopy} C,$$

327

328 where k_{canopy} is the decay rate per year under the closed canopy and C is the closed
329 canopy carbon pool estimate in megagrams of carbon per hectare. Because the
330 percentage of canopy gaps is small, we assumed that the carbon pool estimates from
331 Pfeifer et al. (2015) are representative of the closed canopy. We estimated the carbon
332 flux for our study site, including canopy gaps, using the following equation:

333

334
$$F^* = p k_{gaps} \alpha C + (1 - p) k_{canopy} C,$$

335

336 where F^* is the flux when gaps are included, p is the proportion of canopy gaps at the
337 study site, k_{gaps} , is the decay rate (yr^{-1}) in the canopy gaps and α is the ratio of the
338 volume of dead wood in the canopy gaps to the volume of dead wood under the closed
339 canopy. Because the sample size was small ($n = 4$, each) for the volume of dead wood
340 in the canopy gaps and under the closed canopy, a normal distribution computed from
341 these data may not be reliable. Therefore, we sampled α directly from the dataset for
342 the bootstrapping scheme. Fluxes are reported as geometric means with geometric

343 standard deviation intervals to best represent the central tendency of the
344 approximately log-normal bootstrapped distributions we obtained.

345

346 **Statistical analysis**

347 A linear mixed effect model (R package: *LmerTest*) was used to determine if wood
348 block bag type (macroinvertebrate accessible vs. macroinvertebrate inaccessible),
349 canopy type (closed canopy vs forest gap) and the interaction between the two factors
350 affected proportion of mass lost from wood blocks. Mass loss was logit transformed,
351 which allowed us to use standard Gaussian linear methods (Warton & Hui, 2011) and
352 forest site was included as a random factor. To carry out multiple comparisons of
353 means and identify any differences in wood block mass loss between bag types and
354 canopy types, we used the *glht* function (R package: *multcomp*) and Tukey contrasts.

355 An Adonis test (package: *vegan*) was used to assess if the community composition of
356 termites differed between the closed canopy and forest gap sites, and zero-inflated
357 generalised linear mixed effects models (R package: *glmmTBM*) were used to test for
358 differences in the encounter rate of each genus separately in the closed canopy and
359 forest sites. Linear mixed effects models were used to test for differences in minimum,
360 mean and maximum soil temperature and moisture values in closed canopy and gap
361 sites; forest site and sampling date were included as random factors. Linear mixed
362 models were used to assess the differences in canopy openness between the closed
363 canopy and forest gaps, with site included as a random factor.

364

365 Finally, to model the relationship between termite-derived soil recovered from the
366 woodblocks and woodblock mass loss, while taking into consideration the high

367 proportion of zeros in the data (50% of open woodblocks contained no termite-derived
368 soil), we analysed the data in a two-stage approach following Min & Agresti (2002).
369 First, we created a binomial variable for the termite soil mass, where woodblocks
370 containing no soil received a 0 and those with more than zero grams of soil received
371 a 1. We then fit the data to a generalised linear mixed effect model (glmer) with site
372 included as a random factor, to test if the proportion of wood mass lost (logit
373 transformed) had a significant effect on the probability of a woodblock containing
374 termite soil. Next, we removed the zero soil values from the dataset and ran a linear
375 mixed effects model (lmer) on only woodblocks from which we recovered soil, to
376 assess if logit transformed wood mass loss was significantly associated with the mass
377 of soil that was recovered from the woodblocks. Again, site was included as a random
378 factor. This approach overcame the problem of modelling zero-inflated data (only
379 invertebrate accessible bags were included in these models because no soil was
380 recovered from closed bags).

381

382 **Results**

383 *Decomposition*

384 Significantly more mass was lost from open woodblocks (accessible to both microbes
385 and macroinvertebrates) in forest gaps (mean mass loss over 12 months: $49\% \pm 5\%$)
386 compared with open woodblocks in closed canopy sites (mean mass loss: $30\% \pm 4\%$;
387 $z = 3.8$, $P < 0.001$). This is an increase in decomposition by a factor of 1.63 in forest
388 where both microbes and macroinvertebrates have access to the woodblocks (Fig. 2).
389 In both the closed canopy and gaps sites, the presence of macroinvertebrates
390 significantly increased the proportion of mass lost, but the magnitude of this increase

391 was greater in forest gaps, as indicated by significant interaction between woodblock
392 bag type and canopy type (LRT = 4.18, $P = 0.04$): woodblock mass loss increased by
393 a factor of 2 in open (mean mass loss: $30 \pm 4\%$) compared with closed bags (mean
394 mass loss: $15 \pm 2\%$) in closed canopy sites ($z = 3.08$, $P = 0.01$), but increased by a
395 factor of 2.58 within open (mean mass loss: $49 \pm 5\%$) versus closed bags ($19 \pm 2\%$)
396 in forest gaps ($z = 5.9$, $P < 0.001$). We found a significant positive relationship between
397 woodblock mass loss and the likelihood that a wood block contained termite-derived
398 soil and carton within the open bags ($z = 4.19$, $P < 0.001$; Fig S5), and a significant
399 positive relationship between the proportion of mass lost from a woodblock and the
400 mass of dry soil recovered from bags containing soil ($z = 2.94$, $P = 0.005$; Fig. S5);
401 indicating that termites, rather than other macro-invertebrates, were responsible for
402 this mass loss. There was no significant difference in mass lost from closed
403 woodblocks in the closed canopy compared with closed woodblocks in forest gap sites
404 ($z = 0.86$, $P = 0.83$), suggesting that changes in microbial activity were not responsible
405 for the increase decomposition in the gaps (Fig. 2).

406

407 *Soil microclimate and termite communities*

408 We found small but significant differences in soil temperature and soil moisture within
409 closed canopy and forest gap sites. The soil in gaps tended to be warmer and wetter.
410 Minimum soil temperature was higher by 0.5°C and mean soil temperature was 0.3°C
411 higher in gaps compared with closed canopy sites. There was no significant difference
412 in maximum soil temperature. Minimum, mean and maximum soil moisture were
413 higher in canopy gaps compared with non-gap sites by 2, 1.5 and 3.5 percentage
414 points, respectively (Fig. 3; Table 1). We found no difference in the composition of

415 termite communities collected in the closed canopy compared with forest gaps sites
416 nor was there any difference in the number of encounters of individual genera in the
417 two canopy types (Fig. S6).

418

419 *Gap area and carbon modelling*

420 Within the LiDAR surveyed area of 940 ha of lowland tropical rainforest, we detected
421 a total of 20,928 gaps, with the centre of the cumulative distribution of gaps (i.e. the
422 point where half of the gap area is comprised of smaller gaps and the remaining half
423 by larger gaps) at 122 m² (0.01 ha) and covering a cumulative area of 24 ha, or 2.5%
424 of the study site. Of these, 128 gaps were of comparable size to those used in this
425 study (between 0.025 and 0.16 ha). These gaps covered a cumulative area of 6.5 ha,
426 which is 0.7 % of the surveyed area and represents 27% of the total gap area in the
427 study region (Fig. 4). In the forest matrix immediately surrounding our experimental
428 plots, we found 187% more deadwood in areas affected by tree fall compared with
429 undisturbed areas (average volume in areas more than 20 m from tree fall: 95.4 ± 36.6
430 cm³ per 50 m transect; average volume in areas close to tree fall: 272.9 ± 98.7 cm³
431 per 50 m transect; Fig. 5).

432

433 Our initial model applied the changes in decay rate and wood pools to canopy gaps
434 covering 0.7% of the surveyed area, which is the cumulative area that includes gaps
435 of the same size as those forming the basis of this investigation: 128 gaps in total,
436 measuring between 0.025 and 0.16 ha. Under this assumption of gap area, deadwood
437 carbon fluxes increased above baseline by a geometric mean value of 5.7% with a
438 geometric SD interval of -3.1% to 15.2%, corresponding to a flux increase of 0.09 Mg

439 C ha⁻¹ yr⁻¹ (Table 2). If we assumed changes in wood pools and decay rates applied
440 to all gaps detected by LiDAR, i.e. 2.5% of the survey area, then the flux increase
441 was 18.2% (geometric SD interval of -15.4% to 47.7%), or 0.27 Mg C ha⁻¹ yr⁻¹.
442 Increases in both wood pool sizes and termite-driven decay rates in gaps contributed
443 to the higher fluxes relative to the baseline scenario with no gaps (Fig. S10). At the
444 scale of the 940 ha region of our LiDAR analysis, gap-driven fluxes increased from
445 1380 Mg C ha⁻¹ yr⁻¹ to 1460 Mg C yr⁻¹ for the 0.7% gap scenario and to 1640 Mg C ha⁻¹
446 yr⁻¹ for the 2.5% gap scenario.

447

448 **Discussion**

449 We found that deadwood decomposition in a lowland tropical rainforest increased by
450 approximately two thirds in tree-fall canopy gaps, compared with closed-canopy forest,
451 and that this accelerated decomposition was driven by termites. These results add to
452 a growing body of evidence showing that termites are major drivers of deadwood
453 decomposition in tropical rainforests (Griffiths et al., 2019; Law et al., 2019) and that
454 their importance for the maintenance of ecological processes can increase in response
455 to environmental perturbations (Ashton et al., 2019). The functioning of canopy gaps
456 as hotspots for carbon cycling has important implications for land-surface model
457 development given that tree mortality is increasing in rainforests (Brienen et al., 2015;
458 Hubau et al., 2020; McDowell et al., 2018), which will increase the number of gaps,
459 and cumulative area of forest affected by canopy openings.

460

461

462

463 *Drivers of increased decomposition*

464 We hypothesized that changes in deadwood stocks and microclimate in gaps might
465 alter wood decomposition fluxes. Deadwood stocks were three times higher in canopy
466 gaps than in closed canopy sites. Microbial decomposition did not differ between
467 contrasting canopy conditions while termite-mediated decay increased by almost two
468 thirds in tree-fall gaps. The small but significant differences we detected in the soil
469 microclimate of our gap and closed canopy sites had no effect on microbial decay but
470 may have led to an increase in termite-mediated decay. Combined, these results point
471 to an influx of deadwood foraging material for termites as a likely driver of the
472 increased decomposition in gaps we detected. However, because this hypothesis
473 needs further testing, this work serves as a platform from which the mechanisms
474 behind the patterns we report can be rigorously tested and a starting point for
475 incorporation of these patterns into global carbon models.

476

477 We found no support for our hypothesis that shifts in microclimate and/or disturbance
478 caused by tree mortality are detrimental to the decomposer community. Neither termite
479 nor microbial-mediated wood mass loss declined beneath canopy gaps. Soil
480 conditions in our focal canopy gaps were not as we predicted: although slightly
481 warmer, they were wetter, rather than drier than in the paired closed canopy sites. This
482 result could, in part, explain the lack of disturbance/microclimate effect detected on
483 the decomposer community because we have no *a priori* reason to believe that these
484 small increases in soil moisture would negatively affect microbial or termite activity.

485

486 Our finding of increased termite-mediated decay in canopy gaps supports our
487 alternative hypothesis that an increase in termite food sources (deadwood) in tree fall
488 gaps attracts more termites to these areas, which leads to increased decomposition.
489 We found almost three times more deadwood on the forest floor in areas close to tree
490 fall (Fig. 5), and we propose that this influx of wood is likely to have led to an increase
491 in termite foraging in the gap sites. This finding has important implications for the way
492 in which decomposition models are parameterised in rainforest systems because our
493 results suggest that carbon flux rates from deadwood are not only a function of the
494 proportion of wood necromass in the system (Rice et al., 2004) but may also be
495 mediated by the spatial clustering of the deadwood resource. Given that microbial
496 decay rates did not change in the canopy gaps, we found no evidence to suggest the
497 clustering/influx of dead plant resources had a comparable positive effect on the
498 microbial decomposer community.

499

500 We are confident that termites were responsible for the invertebrate driven increase in
501 decomposition because a previous study, which used macroinvertebrate accessible
502 and inaccessible woodblock bags, in combination with a large-scale suppression of
503 termite communities, demonstrated that non-termite macroinvertebrates do not
504 contribute significantly to wood decay at this site Griffiths et al., (2019). Our present
505 study exactly mimics the experimental design used to manipulate the
506 macroinvertebrate community access to wood blocks in the previous work. Therefore,
507 we conclude that termites were responsible for the elevated mass loss from wood
508 within the macroinvertebrate accessible bags. Moreover, we found a significant
509 positive relationship between the probability that a wood block contained termite-

510 derived soil and proportion wood mass loss, as well as a positive relationship between
511 the mass of soil brought into our open woodblock bags and wood block mass loss (no
512 soil was recovered from closed woodblocks; Fig. S5). This relationship provides further
513 evidence that termites are the main drivers of the observed wood mass loss from the
514 macroinvertebrate accessible bags because termites are the only decomposer
515 organism known to move clay and soil around in this way (Oberst et al., 2016).
516 Because our sampling to assess the composition and biomass of termites within the
517 gap and closed canopy sites was carried out 15-months after the storm that created
518 the focal gaps and influx of deadwood material, it seems likely that we missed the
519 increase in termite activity within the gap sites that we hypothesise led to the elevated
520 decay rate within our gaps. Further work is needed to conclusively disentangle the
521 possible drivers of the increased termite activity and wood decay rates in canopy gaps
522 (microclimate versus increased food supply). Our findings highlight the need to
523 explicitly test the influence of microclimate versus deadwood volume on decay rates
524 in field experiments. This would allow us to gain a deeper understanding of the factors
525 mediating decomposition and carbon balance in rainforest ecosystems.

526

527 *Implications for rainforest carbon flux and sources of uncertainties*

528 We show that termite-mediated deadwood decay responds positively to small-scale
529 disturbances within old-growth rainforest. This suggests that accelerated termite
530 decomposition could be a key driver of observed elevated carbon fluxes caused by
531 increased tree mortality and degradation within standing tropical forests (Baccini et al.,
532 2017; Hubau et al., 2020). As such, these results add to our understanding of the biotic
533 mechanisms underpinning ongoing changes to rainforest carbon budgets. However,

534 the resilience of termite-mediated ecosystem processes to differing disturbance
535 thresholds is largely unknown (but see Tuma *et al.* 2019). Recent work has shown that
536 termites maintain leaf litter decomposition, nutrient heterogeneity and soil moisture
537 retention in old growth forest during periods of drought (Ashton *et al.*, 2019), indicating
538 that they can provide ecosystem resilience to climate change. Understanding the
539 extent to which the resilience provided by termites is maintained in degraded habitats
540 is key to the on-going improvement of land-surface models as well the development
541 of land-management practices aimed at increasing the resilience of tropical
542 landscapes under ongoing environmental change

543

544 Given the vast amounts of carbon contained within tropical forests (Lewis, Edwards,
545 & Galbraith, 2015; Pan *et al.*, 2011), even a relatively small change in C flux due to
546 termite-mediated decomposition in canopy gaps may scale up to large differences
547 over tropical biomes. For example, our estimated flux increase of $0.27 \text{ Mg C ha}^{-1} \text{ yr}^{-1}$
548 represents 2% of total net primary productivity ($13.5 \text{ Mg C ha}^{-1} \text{ yr}^{-1}$) measured in
549 lowland rainforests of Malaysian Borneo (Riutta *et al.*, 2018). This timely finding is of
550 particular relevance given that the Community Land Model version 6 (CLM6) is
551 currently under development, which will include additional parameterisation of
552 ecosystem processes that influence the cycling of C through terrestrial ecosystems
553 and build upon progress made in CLM5 (Lawrence *et al.*, 2019). However, although
554 our analysis indicated the potential for substantial increases in carbon flux due to
555 changes in termite activity in canopy gaps, the variance around the estimated
556 magnitude of this change in flux remains high due to a number of potential sources of
557 uncertainty in our model.

558

559 Lack of data on how climate mediates the relationship between termite-driven decay
560 and wood density represents an area of uncertainty in our model estimates and
561 contributes to the large confidence intervals associated with our C-flux estimates. Our
562 estimate of termite-mediated decay associated with the varying wood densities is
563 reliant on an empirical model we fitted to a single dataset of decay rates from a distant
564 study site in Yunnan Province, China (Liu et al., 2015). While both are Asian tropical
565 rainforests, the climate differs between the two regions: mean annual rainfall of 1463
566 mm versus 2838 mm and average monthly temperatures of 21.7°C versus 24.9°C in
567 Yunan (Li et al., 2012) and Maliau (Law et al., 2019), respectively. These climatic
568 differences could be important because while some studies suggest that wood traits
569 are key drivers of deadwood decay (Hu et al., 2018; Zanne et al., 2015), others have
570 found stronger relationships with climate (Chambers, Higuchi, Schimel, Ferreira, &
571 Melack, 2000; Pietsch et al., 2019). Consequently, it is possible that the effect of wood
572 density on rate of termite mediated decay could differ between the two regions.

573

574 Wood density is not the only trait known to influence decay rates. Results from studies
575 focussed on microbial wood decomposition in temperate regions show that a range of
576 other traits can also significantly effect wood decay, either positively (e.g.
577 phosphorous, nitrogen) or negatively (e.g. bark ratio, lignin concentration [Kahl et al.,
578 2017; Oberle et al., 2019]). Furthermore, a recent meta-analysis (Hu et al., 2018),
579 highlighted the importance of wood size (diameter) and nitrogen concentration in
580 controlling wood decay globally. We acknowledge that termite-mediated decay rates
581 could also be influenced by these wood traits and our models may be improved if more

582 data were available on the effect of wood stoichiometry on termite attack rate in our
583 system. However, data on wood chemical traits within our study region are currently
584 unavailable, but Martin, Erickson, Kress, & Thomas (2014) provide an overview of
585 wood nitrogen concentration and correlations between nitrogen and other wood traits
586 for 59 Panamanian tree species. This work reveals a mean wood C:N ratio for these
587 neo-tropical tree species of 278 ± 32 , with values ranging from 84.7 to 1360.8, and a
588 positive relationship between wood density and wood nitrogen concentration. Our
589 wood decomposition substrate (*Pinus radiata*) falls within this range with a C:N of 462
590 (Ganjegunte et al., 2004).

591

592 We are aware of no study that has interrogated the influence of wood chemical traits
593 on termite mediated decomposition; therefore, we are unable to speculate as to how
594 these factors could influence our flux estimate. However, Ulyshen, Müller, & Seibold
595 (2016) show that termite-mediated wood mass loss increased significantly where bark
596 was present, which is in contrast to the findings presented by Kahl et al., (2017) who
597 show that higher bark ratio negatively affected microbial decay rates. It is important to
598 note that our use of wood blocks of a uniform (small) size and lacking in bark could
599 have resulted in elevated mass loss compared to larger woody substrates with intact
600 bark. However, our wood substrate was chosen to allow for standardization and to
601 facilitate comparison across our experimental sites and treatments. Therefore, we
602 highlight the need for additional work to partition the contributions of microbes versus
603 termites in the decomposition of deadwood with a range of traits and in a range of
604 ecosystems to facilitate the development of more precise models of wood
605 decomposition and carbon cycling.

606

607 Possible inaccuracies in our estimates of deadwood on the forest floor are another
608 potential source of error in our model estimates. We reported that the volume of
609 deadwood was 187% higher in areas affected by treefall compared with those
610 unaffected, using field transects 5-months after the storm that created the canopy
611 gaps. However, it is possible that termite-mediated wood removal in that 5-month
612 period, in response to the influx of foraging material, removed deadwood
613 disproportionately from the tree-fall sites. This would result in an underestimation of
614 the difference in wood volume in contrasting canopy environments, with potentially
615 more deadwood in recently created gaps than we reported. Further, we used data
616 from Pfeifer *et al.* (2015) to describe the deadwood carbon pool under closed canopy
617 conditions. However, Pfeifer *et al.* (2015) reported different deadwood carbon
618 estimates from two sites, both within 3.2 km of our study site (“OG1”: 27.05 Mg C per
619 ha, and “OG2”: 10.24 Mg per ha). We used values from the site closest to our
620 experimental plots (< 1km), OG 2, which was the lowest carbon pool value and thus
621 avoids inflated estimates of the effect of termites on regional C flux. However, the
622 higher deadwood carbon pool reported from Old Growth 1 combined with the
623 possibility that we underestimated the proportional difference in deadwood volume in
624 gaps versus closed canopy sites suggests that our modelling effort is a conservative
625 estimate of the true effect of termite mediated C flux in canopy gaps.

626

627 Finally, difficulties in describing temporally and spatially representative forest canopy
628 gap fractions may have contributed model inaccuracies. Using data from the aerial
629 survey carried out in November 2014, we found the cumulative area of canopy gaps

630 in the study region to be between 0.7 and 2.5%. This range is within the lower bounds
631 of canopy gap fractions described by Hunter *et al.* (2015) in the Amazon rainforest (2-
632 5%) and smaller than that reported by Yavitt *et al.* (1995) within a Panamanian forest
633 (4%). Small canopy openings in rainforest ecosystems caused by isolated tree fall
634 events rapidly become colonised by lateral canopy growth, meaning that their
635 detectability using remote sensing quickly decreases with time since gap creation
636 (Asner, Keller, & Silva, 2004). The aerial survey used in this investigation was not, as
637 far as we are aware, carried out soon after an intense storm similar to the storm that
638 created the focal gaps in this study. Therefore, our gap fraction estimate is likely to be
639 smaller than if it been carried out immediately following the storm that formed the basis
640 of this investigation. However, despite these uncertainties, our analysis demonstrates
641 that canopy gaps in rainforest ecosystems function as hotspots of deadwood decay,
642 which has far reaching implications for regional and global budgeting.

643

644 *Conclusion*

645 To our knowledge, this is the first study to show that rainforest treefall canopy gaps
646 represent hotspots for deadwood decay and carbon cycling. We provide insights into
647 the relative importance of invertebrates compared with microbes in driving the
648 decomposition of deadwood, adding to a growing body of literature showing that
649 termites and their mutualistic microbes are equally, if not more important than free-
650 living microorganisms for deadwood decay in rainforests (Griffiths *et al.*, 2019; Law *et*
651 *al.*, 2019). These results demonstrate that to improve the accuracy of carbon
652 modelling, a variable rate of decomposition should be included in model parameters
653 to account for accelerated termite-mediated decay within tree fall canopy gaps.

654 However, we urgently require information on the effect of a variety of wood traits on
655 termite-mediated decay rates, as well as research efforts to quantify whether these
656 patterns of accelerated decomposition hold true in selectively logged forest or oil palm
657 plantations. Only through addressing these knowledge gaps will we be able to reduce
658 model uncertainties and accurately predict how ongoing changes to tropical
659 landscapes will affect global carbon cycling, climate and the functioning and
660 maintenance of vitally important tropical rainforest ecosystems.

661

662 **Acknowledgements**

663 We are extremely grateful to our field assistants R. Binti Manber, Lawlina Mansul and
664 Donny Banasib for their tireless hard work in the field, which made this study possible.
665 We thank G. Reynolds, U. Jami and A. Karolus for coordinating fieldwork. This work
666 was supported by the South East Asian Rainforest Research Partnership (SEARRP),
667 with permission from Maliau Basin Management Committee and the Sabah
668 Biodiversity Council. We thank the funding bodies that financially supported this work:
669 The Leverhulme Trust, research grant: RPG-2017-271 awarded to KP; National
670 Science Foundation, Research Traineeship 1633631 to NHS, and National Science
671 Foundation, grant DEB-1655340 to SDA.

672

673 **Data Sharing and Accessibility**

674 The data that support the findings of this study are openly available in Dryad data
675 repository at [http://doi.org/\[doi\]](http://doi.org/[doi]), reference number [reference number].

676

677 **References**

678 Allen, C. D., Breshears, D. D., & McDowell, N. G. (2015). On underestimation of
679 global vulnerability to tree mortality and forest die-off from hotter drought in the
680 Anthropocene. *Ecosphere*, 6(8), 1–55. <https://doi.org/10.1890/ES15-00203.1>

681 Ashton, L. A., Griffiths, H. M., Parr, C. L., Evans, T. A., Didham, R. K., Hasan, F., ...
682 Eggleton, P. (2019). Termites mitigate the effects of drought in tropical
683 rainforest. *Science*, 177(January), 174–177.

684 Asner, G. P., Keller, M., & Silva, J. N. M. (2004). Spatial and temporal dynamics of
685 forest canopy gaps following selective logging in the eastern Amazon. *Global
686 Change Biology*, 10(5), 765–783. [https://doi.org/10.1111/j.1529-
8817.2003.00756.x](https://doi.org/10.1111/j.1529-
687 8817.2003.00756.x)

688 Baccini, A., Walker, W., Carvalho, L., Farina, M., Sulla-Menashe, D., & Houghton, R.
689 A. (2017). Tropical forests are a net carbon source based on aboveground
690 measurements of gain and loss. *Science*, 358(October), 230–234.

691 Blonder, B., Both, S., Coomes, D. A., Elias, D., Jucker, T., Kvasnica, J., ... Svátek,
692 M. (2018). Extreme and Highly Heterogeneous Microclimates in Selectively
693 Logged Tropical Forests. *Frontiers in Forests and Global Change*, 1(October),
694 1–14. <https://doi.org/10.3389/ffgc.2018.00005>

695 Bodman, R. W., Rayner, P. J., & Karoly, D. J. (2013). Uncertainty in temperature
696 projections reduced using carbon cycle and climate observations. *Nature
697 Climate Change*, 3(8), 725–729. <https://doi.org/10.1038/nclimate1903>

698 Brien, R. J. W., Phillips, O. L., Feldpausch, T. R., Gloor, E., Baker, T. R., Lloyd, J.,
699 ... Zagt, R. J. (2015). Long-term decline of the Amazon carbon sink. *Nature*,
700 519(7543), 344–348. <https://doi.org/10.1038/nature14283>

701 Cai, W., Borlace, S., Lengaigne, M., Van Renssch, P., Collins, M., Vecchi, G., ... Jin,

702 F. F. (2014). Increasing frequency of extreme El Niño events due to greenhouse
703 warming. *Nature Climate Change*, 4(2), 111–116.

704 <https://doi.org/10.1038/nclimate2100>

705 Carlson, B. S., Koerner, S. E., Medjibe, V. P., White, L. J. T., & Poulsen, J. R.
706 (2017). Deadwood stocks increase with selective logging and large tree
707 frequency in Gabon. *Global Change Biology*, 23(4), 1648–1660.
708 <https://doi.org/10.1111/gcb.13453>

709 Chambers, J. Q., Higuchi, N., Schimel, J. P., Ferreira, L. V., & Melack, J. M. (2000).
710 Decomposition and carbon cycling of dead trees in tropical forests of the central
711 Amazon. *Oecologia*, 122(3), 380–388. <https://doi.org/10.1007/s004420050044>

712 Cornwell, W. K., Cornelissen, J. H. C., Allison, S. D., Bauhus, J., Eggleton, P.,
713 Preston, C. M., ... Zanne, A. E. (2009). Plant traits and wood fates across the
714 globe: Rotted, burned, or consumed? *Global Change Biology*, 15(10), 2431–
715 2449. <https://doi.org/10.1111/j.1365-2486.2009.01916.x>

716 da Costa, R. R., Hu, H., Li, H., & Poulsen, M. (2019). Symbiotic plant biomass
717 decomposition in Fungus-Growing termites. *Insects*, 10(4), 1–15.
718 <https://doi.org/10.3390/insects10040087>

719 Dibog, L., Eggleton, P., Norgrove, L., Bignell, D. E., & Hauser, S. (1999). Impacts of
720 canopy cover on soil termite assemblages in an agrisilvicultural system in
721 southern Cameroon. *Bulletin of Entomological Research*, 89(02), 125–132.
722 <https://doi.org/10.1017/S0007485399000206>

723 Eggleton, P., Bignell, D. E., Sands, W. A., Waite, B., Wood, T. G., & Lawton, J. H.
724 (1995). The species richness of termites (Isoptera) under differing levels of
725 forest disturbance in the mbalmayo forest reserve, southern cameroon. *Journal*

726 *of Tropical Ecology*, 11(1), 85–98. <https://doi.org/10.1017/S0266467400008439>

727 Ewers, R. M., Boyle, M. J. W., Gleave, R. A., Plowman, N. S., Benedick, S., Bernard,

728 H., ... Turner, E. C. (2015). Logging cuts the functional importance of

729 invertebrates in tropical rainforest. *Nature Communications*, 6, 6836.

730 <https://doi.org/10.1038/ncomms7836>

731 Ganjegunte, G. K., Condron, L. M., Clinton, P. W., Davis, M. R., & Mahieu, N.

732 (2004). Decomposition and nutrient release from radiata pine (*Pinus radiata*)

733 coarse woody debris. *Forest Ecology and Management*, 187(2–3), 197–211.

734 [https://doi.org/10.1016/S0378-1127\(03\)00332-3](https://doi.org/10.1016/S0378-1127(03)00332-3)

735 Griffiths, H. M., Ashton, L. A., Evans, T. A., Parr, C. L., & Eggleton, P. (2019).

736 Termites can decompose more than half of deadwood in tropical rainforest.

737 *Current Biology*, 29, 118–119. <https://doi.org/10.1016/j.cub.2019.01.012>

738 Hardwick, S. R., Toumi, R., Pfeifer, M., Turner, E. C., Nilus, R., & Ewers, R. M.

739 (2015). The relationship between leaf area index and microclimate in tropical

740 forest and oil palm plantation: Forest disturbance drives changes in

741 microclimate. *Agricultural and Forest Meteorology*, 201, 187–195.

742 <https://doi.org/10.1016/j.agrformet.2014.11.010>

743 Harmon, M. E., Bond-Lamberty, B., Tang, J., & Vargas, R. (2011). Heterotrophic

744 respiration in disturbed forests: A review with examples from North America.

745 *Journal of Geophysical Research: Biogeosciences*, 116(2), 1–17.

746 <https://doi.org/10.1029/2010JG001495>

747 Harmon, M. E., Fasth, B. G., Yatskov, M., Kastendick, D., Rock, J., & Woodall, C. W.

748 (2020). Release of coarse woody detritus - related carbon : a synthesis across

749 forest biomes. *Carbon Balance and Management*, 1–21.

750 <https://doi.org/10.1186/s13021-019-0136-6>

751 Hu, Z., Michaletz, S. T., Johnson, D. J., McDowell, N. G., Huang, Z., Zhou, X., & Xu, C. (2018). Traits drive global wood decomposition rates more than climate.

752 *Global Change Biology*, 24(11), 5259–5269. <https://doi.org/10.1111/gcb.14357>

753

754 Hubau, W., Lewis, S. L., Phillips, O. L., Affum-Baffoe, K., Beeckman, H., Cuní-

755 Sanchez, A., ... Zemagho, L. (2020). Asynchronous carbon sink saturation in

756 African and Amazonian tropical forests. *Nature*, 579(7797), 80–87.

757 <https://doi.org/10.1038/s41586-020-2035-0>

758 Hunter, M. O., Keller, M., Morton, D., Cook, B., Lefsky, M., Ducey, M., ... Zang, R.

759 (2015). Structural dynamics of tropical moist forest gaps. *PLoS ONE*, 10(7), 1–

760 19. <https://doi.org/10.1371/journal.pone.0132144>

761 Jackson, T. ., Shenkin, A. ., Majalap, N., Jami, J. ., Sailim, A. B., Reynolds, G., ...

762 Disney, M. (2020). The mechanical stability of the world's tallest broadleaf trees.

763 *The Mechanical Stability of the World's Tallest Broadleaf Trees*, 00, 1–11.

764 <https://doi.org/10.1101/664292>

765 Janisch, J. E., Harmon, M. E., Chen, H., Fasth, B., & Sexton, J. (2005).

766 Decomposition of coarse woody debris originating by clearcutting of an old-

767 growth conifer forest. *Écoscience*, 12(2), 151–160.

768 <https://doi.org/10.2980/i1195-6860-12-2-151.1>

769 Jones, D. T., & Eggleton, P. (2000). Sampling termite assemblages in tropical

770 forests: Testing a rapid biodiversity assessment protocol. *Journal of Applied*

771 *Ecology*, 37(1), 191–203. <https://doi.org/10.1046/j.1365-2664.2000.00464.x>

772 Kahl, T., Arnstadt, T., Baber, K., Bässler, C., Bauhus, J., Borken, W., ... Gossner, M.

773 M. (2017). Wood decay rates of 13 temperate tree species in relation to wood

774 properties, enzyme activities and organismic diversities. *Forest Ecology and*
775 *Management*, 391, 86–95. <https://doi.org/10.1016/j.foreco.2017.02.012>

776 Law, S., Eggleton, P., Griffiths, H., Ashton, L., & Parr, C. (2019). Suspended Dead
777 Wood Decomposes Slowly in the Tropics , with Microbial Decay Greater than
778 Termite Decay. *Ecosystems*, (June). <https://doi.org/10.1007/s10021-018-0331-4>

779 Lawrence, D. M., Fisher, R. A., Koven, C. D., Oleson, K. W., Swenson, S. C., Bonan,
780 G., ... Zeng, X. (2019). The Community Land Model Version 5: Description of
781 New Features, Benchmarking, and Impact of Forcing Uncertainty. *Journal of*
782 *Advances in Modeling Earth Systems*, 11(12), 4245–4287.
783 <https://doi.org/10.1029/2018MS001583>

784 Lewis, S. L., Edwards, D. P., & Galbraith, D. (2015). Increasing human dominance of
785 tropical forests. *Science*, 349, 827–832.

786 Li, R., Luo, G., Meyers, P. A., Gu, Y., Wang, H., & Xie, S. (2012). Leaf wax n-alkane
787 chemotaxonomy of bamboo from a tropical rain forest in Southwest China. *Plant*
788 *Systematics and Evolution*, 298(4), 731–738. <https://doi.org/10.1007/s00606-011-0584-2>

790 Liu, G., Cornwell, W. K., Cao, K., Hu, Y., Van, R. S. P., Yang, S., ... Cornelissen, J.
791 H. C. (2015). Termites amplify the effects of wood traits on decomposition rates
792 among multiple bamboo and dicot woody species. *Journal of Ecology*, 103,
793 1214–1223. <https://doi.org/10.1111/1365-2745.12427>

794 Luke, S. H., Fayle, T. M., Eggleton, P., Turner, E. C., & Davies, R. G. (2014).
795 Functional structure of ant and termite assemblages in old growth forest, logged
796 forest and oil palm plantation in Malaysian Borneo. *Biodiversity and*
797 *Conservation*, 23(11), 2817–2832. <https://doi.org/10.1007/s10531-014-0750-2>

798 Lyu, M., Xie, J., Vadeboncoeur, M. A., Wang, M., Qiu, X., Ren, Y., ... Kuzyakov, Y.
799 (2018). Simulated leaf litter addition causes opposite priming effects on natural
800 forest and plantation soils. *Biology and Fertility of Soils*, 54(8), 925–934.
801 <https://doi.org/10.1007/s00374-018-1314-5>

802 Martin, A. R., Erickson, D. L., Kress, W. J., & Thomas, S. C. (2014). Wood nitrogen
803 concentrations in tropical trees: phylogenetic patterns and ecological correlates.
804 *New Phytologist*, 205, 484–495.

805 McDowell, N., Allen, C. D., Anderson-Teixeira, K., Brando, P., Brienen, R.,
806 Chambers, J., ... Xu, X. (2018). Drivers and mechanisms of tree mortality in
807 moist tropical forests. *New Phytologist*, 219(3), 851–869.
808 <https://doi.org/10.1111/nph.15027>

809 Min, Y., & Agresti, A. (2002). Modeling Nonnegative Data with Clumping at Zero : A
810 Survey Models for Semicontinuous Data. *Jirss*, 1(May), 7–33.

811 Mori, S., Itoh, A., Nanami, S., Tan, S., Chong, L., & Yamakura, T. (2014). Effect of
812 wood density and water permeability on wood decomposition rates of 32
813 bornean rainforest trees. *Journal of Plant Ecology*, 7(4), 356–363.
814 <https://doi.org/10.1093/jpe/rtt041>

815 Newbery, D. M., & Lingenfelder, M. (2004). Resistance of a lowland rain forest to
816 increasing drought intensity in Sabah, Borneo. *Journal of Tropical Ecology*,
817 20(6), 613–624. <https://doi.org/10.1017/S0266467404001750>

818 Oberle, B., Lee, M. R., Myers, J. A., Osazuwa-Peters, O. L., Spasojevic, M. J.,
819 Walton, M. L., ... Zanne, A. E. (2020). Accurate forest projections require long-
820 term wood decay experiments because plant trait effects change through time.
821 *Global Change Biology*, 26(2), 864–875. <https://doi.org/10.1111/gcb.14873>

822 Oberle, B., Lee, M. R., Myers, J. A., Osazuwa-Peters, O. L., Spasojevic, M. J.,
823 Walton, M. L., ... Zanne, A. E. (2019). Accurate forest projections require long-
824 term wood decay experiments because plant trait effects change through time.
825 *Global Change Biology*, (October), 1–12. <https://doi.org/10.1111/gcb.14873>

826 Oberst, S., Lai, J. C. S., & Evans, T. A. (2016). Termites utilise clay to build structural
827 supports and so increase foraging resources. *Scientific Reports*, 6(September
828 2015), 1–11. <https://doi.org/10.1038/srep20990>

829 Pan, Y., Birdsey, R. a, Fang, J., Houghton, R., Kauppi, P. E., Kurz, W. a, ... Hayes,
830 D. (2011). A large and persistent carbon sink in the world's forests. *Science*,
831 333(6045), 988–993. <https://doi.org/10.1126/science.1201609>

832 Pfeifer, M., Lefebvre, V., Turner, E., Cusack, J., Khoo, M. S., Chey, V. K., ... Ewers,
833 R. M. (2015). Deadwood biomass: An underestimated carbon stock in degraded
834 tropical forests? *Environmental Research Letters*, 10(4).
835 <https://doi.org/10.1088/1748-9326/10/4/044019>

836 Pietsch, K. A., Eichenberg, D., Nadrowski, K., Bauhus, J., Buscot, F., Purahong, W.,
837 ... Wirth, C. (2019). Wood decomposition is more strongly controlled by
838 temperature than by tree species and decomposer diversity in highly species
839 rich subtropical forests. *Oikos*, 128(5), 701–715.
840 <https://doi.org/10.1111/oik.04879>

841 Rice, A. H., Pyle, E. H., Saleska, S. R., Hutyra, L., Palace, M., Keller, M., ... Wofsy,
842 S. C. (2004). Carbon balance and vegetation dynamics in an old-growth
843 Amazonian forest. *Ecological Applications*, 14(4), 55–71.
844 <https://doi.org/10.1890/02-6006>

845 Riutta, T., Malhi, Y., Kho, L. K., Marthews, T. R., Huaraca Huasco, W., Khoo, M. S.,

846 ... Ewers, R. M. (2018). Logging disturbance shifts net primary productivity and
847 its allocation in Bornean tropical forests. *Global Change Biology*, 24(7), 2913–
848 2928. <https://doi.org/10.1111/gcb.14068>

849 Shorohova, E., & Kapitsa, E. (2014). Influence of the substrate and ecosystem
850 attributes on the decomposition rates of coarse woody debris in European
851 boreal forests. *Forest Ecology and Management*, 315, 173–184.
852 <https://doi.org/10.1016/j.foreco.2013.12.025>

853 Stoklosa, A. M., Ulyshen, M. D., Fan, Z., Varner, M., Seibold, S., & Müller, J. (2016).
854 Effects of mesh bag enclosure and termites on fine woody debris decomposition
855 in a subtropical forest. *Basic and Applied Ecology*, 17(5), 463–470.
856 <https://doi.org/10.1016/j.baae.2016.03.001>

857 Swift, M. J. (1977). The ecology of wood decomposition. *Science Progress*, 64(254),
858 175–199. Retrieved from
859 <http://www.bcin.ca/Interface/openbcin.cgi?submit=submit&Chinkey=35034>

860 Swinfield, T., Both, S., Riutta, T., Bongalov, B., Elias, D., Majalap-Lee, N., ...
861 Coomes, D. (2019). Imaging spectroscopy reveals the effects of topography and
862 logging on the leaf chemistry of tropical forest canopy trees. *Global Change
863 Biology*, (October), 1–14. <https://doi.org/10.1111/gcb.14903>

864 Tuma, J., Fleiss, S., Eggleton, P., Frouz, J., Klimes, P., Lewis, O. T., ... Fayle, T. M.
865 (2019). Logging of rainforest and conversion to oil palm reduces bioturbator
866 diversity but not levels of bioturbation. *Applied Soil Ecology*, 144(August), 123–
867 133. <https://doi.org/10.1016/j.apsoil.2019.07.002>

868 Ulyshen, M. D., Müller, J., & Seibold, S. (2016). Bark coverage and insects in fl
869 uence wood decomposition : Direct and indirect effects. *Applied Soil Ecology*,

870 105, 25–30. <https://doi.org/10.1016/j.apsoil.2016.03.017>

871 Van Wagner C.E. (1968). The Line Intersect Method in Forest Fuel Sampling. *Forest*
872 *Science*, 14(1), 20–26.

873 Warton, D. I., & Hui, F. K. C. (2011). The arcsine is asinine: the analysis of
874 proportions in ecology. *Ecology*, 92(1), 3–10.

875 Yavitt, J. B., Battles, J. J., Lang, G. E., & Knight, D. H. (1995). The Canopy Gap
876 Regime in a Secondary Neotropical Forest in Panama. *Journal of Tropical*
877 *Ecology*, 11(3), 391–402.

878 Yavitt, J. B., Wright, S. J., & Wieder, R. K. (2004). Seasonal drought and dry-season
879 irrigation influence leaf-litter nutrients and soil enzymes in a moist, lowland
880 forest in Panama. *Austral Ecology*, 29(2), 177–188.
881 <https://doi.org/10.1111/j.1442-9993.2004.01334.x>

882 Zanne, A. E., Lopez-Gonzalez, G., Coomes, D. A., Llic, J., Jansen, S., Lewis, S. L.,
883 ... Chave, J. (2009). Global wood density database. *Dryad*.

884 Zanne, A. E., Oberle, B., Dunham, K. M., Milo, A. M., Walton, M. L., & Young, D. F.
885 (2015). A deteriorating state of affairs: How endogenous and exogenous factors
886 determine plant decay rates. *Journal of Ecology*, 103(6), 1421–1431.
887 <https://doi.org/10.1111/1365-2745.12474>

888

889

890

891

892

893

894 **Tables**

895 **Table 1.** Mean soil temperature and moisture in closed canopy and forest gap sites
 896 and outputs from linear mixed effects models to assess the effect of gaps on soil
 897 conditions (asterisks indicate significant differences between closed canopy and gap
 898 sites).

Microclimate metric	Mean value		t-value	P
	Closed canopy	Forest gap		
Min. soil temp. (°C)	22.77	± 0.22	23.25	± 0.17
Mean soil temp. (°C)	24.09	± 0.07	24.40	± 0.07
Max soil temp. (°C)	25.13	± 0.10	25.38	± 0.09
Min. soil moisture (%)	12.90	± 0.39	14.06	± 0.24
Mean soil moisture (%)	19.50	± 0.44	20.95	± 0.48
Max soil moisture (%)	26.77	± 0.58	30.26	± 0.76

899

900

901

902

903

904

905

906

907

908

909

910

911 **Table 2.** Estimates of geometric mean carbon fluxes and standard deviation intervals
912 (square brackets) based on 1×10^6 simulations for the following scenarios: a closed
913 canopy baseline; a scenario with 0.7% forest gap, which, based on the LiDAR data, is
914 the cumulative percentage of forest area that is a gap of the same size as our focal
915 experimental gaps (between 0.025 and 0.16 ha); and a scenario with 2.5% forest gap,
916 which is the total (maximum) proportion of forest that was classified as a gap in the
917 LiDAR survey.

	Baseline	0.7% Forest gaps	2.5% Forest gaps
Carbon flux (Mg C ha ⁻¹ yr ⁻¹)	1.47 [0.57, 3.83]	1.56 [0.61, 3.96]	1.74 [0.70, 4.32]
Ratio to baseline	1.000	1.057 [0.969, 1.152]	1.182 [0.846, 1.477]
Carbon flux for LiDAR region (Mg C yr ⁻¹)	1380 [530, 3600]	1460 [570, 3720]	1640 [660, 4060]

918

919

920 **Figure legends**

921

922 **Figure 1.** Schematic diagram of the study experimental design. In October 2017, we
923 selected 10 canopy gaps (mean width 24.5 m, mean length 32 m), created by tree-
924 fall during a storm even in July 217, and 10 paired closed canopy sites (located 20 m
925 from the edge of each gap). Within each gap and closed canopy site, we randomly
926 placed 5 x invertebrate accessible woodblocks (represented by the grey boxes) and
927 5 x invertebrate inaccessible woodblock (yellow boxes). Each woodblock was
928 separated by at least 5 m and was left on the forest floor for 12-months.

929

930 **Figure 2.** Median plus interquartile range for mass loss from macroinvertebrate
931 accessible (grey boxes) and macroinvertebrate inaccessible (yellow boxes) wood
932 blocks within closed canopy and tree-fall gaps. Points are the raw data are displayed
933 over the boxes.

934

935 **Figure 3.** Frequency distributions of minimum, mean and maximum soil temperature
936 (panels a, c, e) and soil moisture (panels b, d, f) within closed canopy (grey ribbons)
937 and forest gaps (yellow ribbons). Vertical dashed lines indicate significant differences
938 between mean microclimate attributes in the different canopy types (closed canopy:
939 grey lines, forest gaps: yellow lines).

940

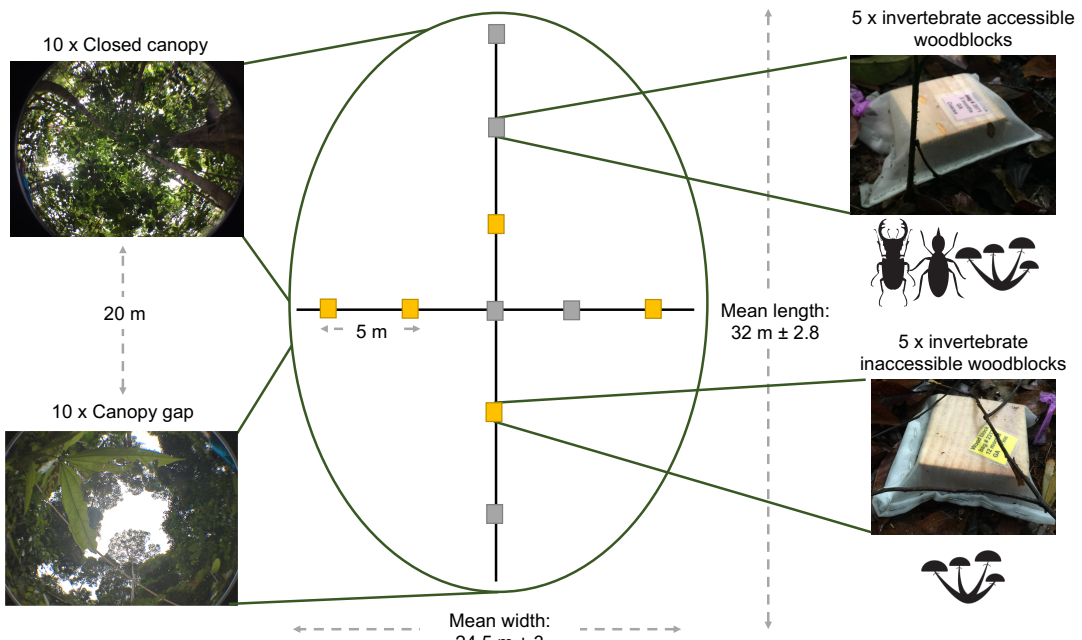
941 **Figure 4.** Cumulative distribution of canopy gap area. Gaps of the same area as those
942 forming the basis of this investigation (128 gaps, between 0.025 and 0.16 ha) fall within
943 the yellow rectangle. The total area represented by the yellow rectangle is 6.5 ha,
944 which is 0.7 % of the surveyed area and represents 27% of the total gap area in the
945 study region. The vertical dashed line at 122 m² (0.01 ha) represents the centre of the
946 cumulative distribution function, where half of the gap area is comprised of smaller
947 gaps and the remaining half by larger gaps.

948

949 **Figure 5.** Median (horizontal lines) plus 95% confidence intervals (whiskers) of the
950 volume of deadwood on the forest floor beneath closed canopy (grey box) and sites
951 within 5 m of a canopy gap.

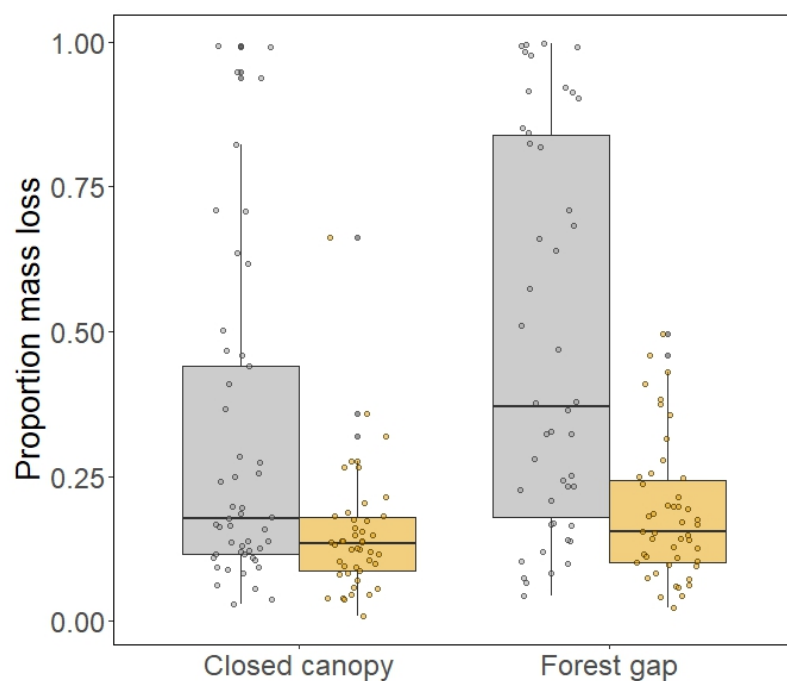
952

953



954

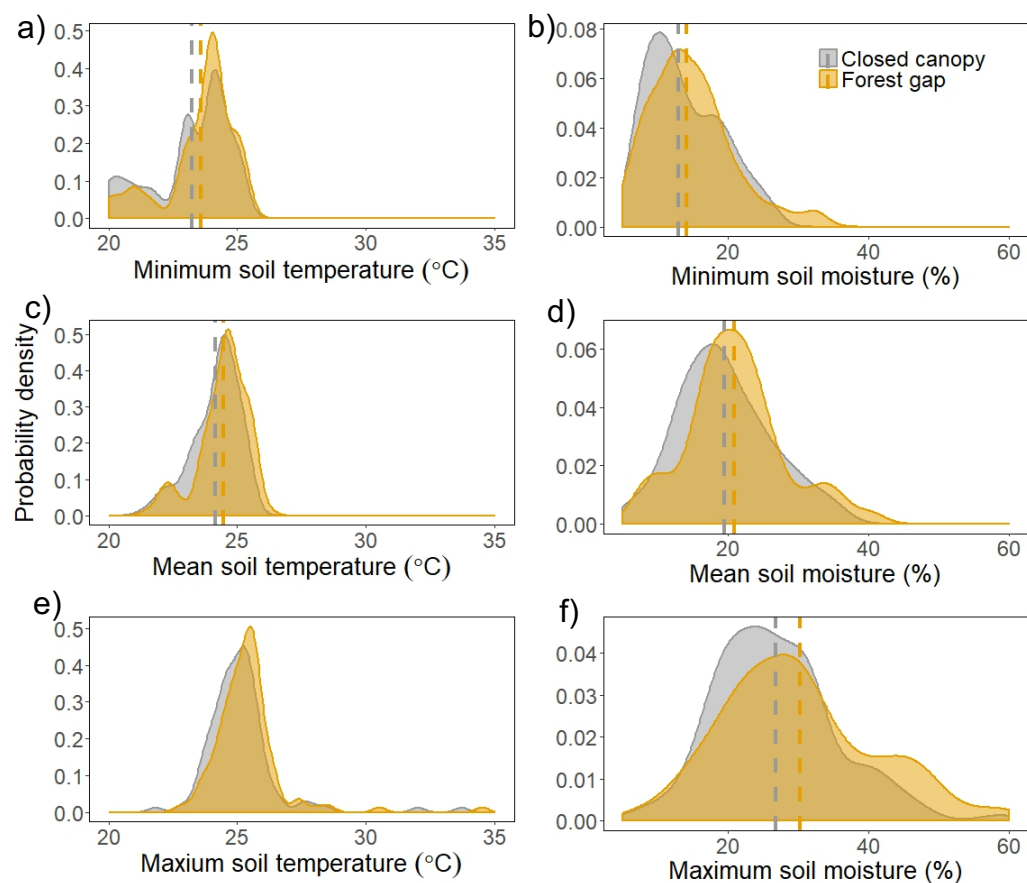
955 **Figure 1.**



956

957 **Figure 2.**

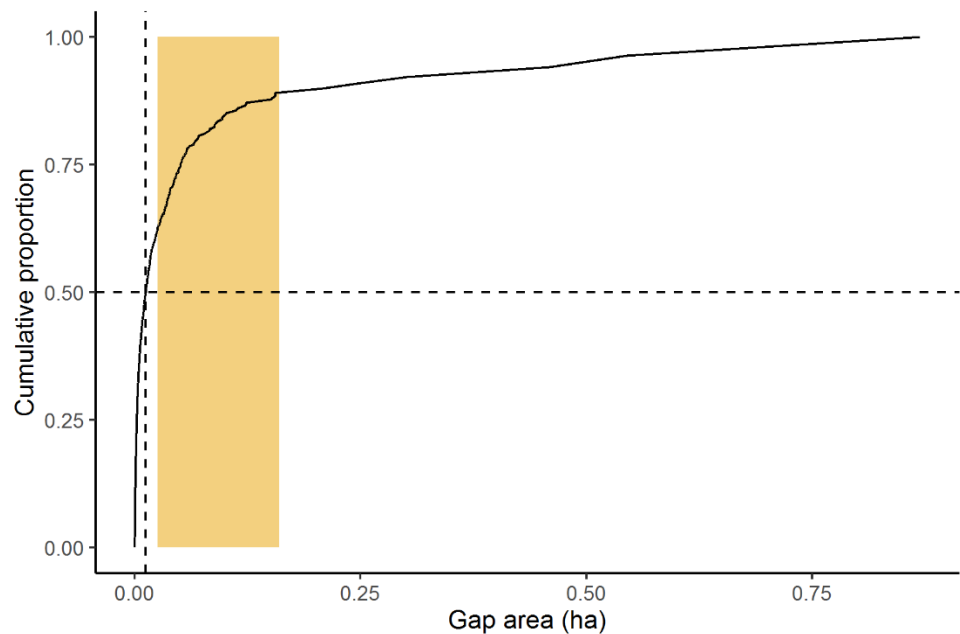
958



959

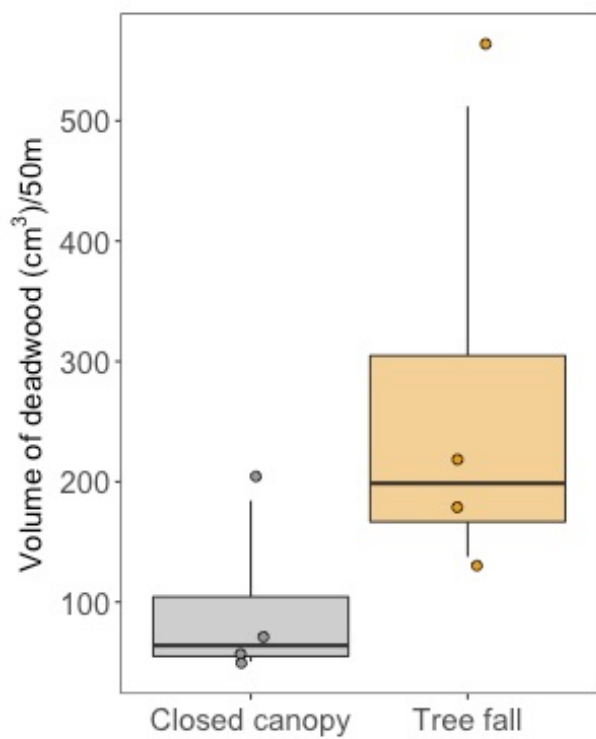
960 **Figure. 3**

961



962

963 **Figure 4.**



964

965 **Figure 5.**